Atmospheric
Chemistry
and Physics
Discussions

Gaseous elemental mercury (GEM) fluxes over canopy of two typical subtropical forests in south China

Qian Yu[1], Yao Luo[1], Shuxiao Wang[1,2], Zhiqi Wang[1], Jiming Hao[1,2], Lei Duan[1,2]

[1]State Key Laboratory of Environmental Simulation and Pollution Control, School of Environment, Tsinghua University, Beijing 100084, China.
[2]Collaborative Innovation Centre for Regional Environmental Quality, Tsinghua University, Beijing 100084, China.

Correspondence to: Lei Duan (lduan@tsinghua.edu.cn)

Abstract. Mercury (Hg) exchange between forests and the atmosphere plays an important role in global Hg cycling. The present estimate of global emission of Hg from natural source has large uncertainty partly due to the lack of chronical and valid field data, particularly for terrestrial surfaces in China, the most important contributor to global atmospheric Hg. In this study, micrometeorological method (MM) was used to continuously observe gaseous elemental mercury (GEM) fluxes over forest canopy at a clean site (Qianyanzhou, QYZ) and a contaminated site (Huitong, HT, near a large Hg mine) in subtropical south China for a full year from January to December in 2014. The GEM flux measurements over forest canopy in QYZ and HT showed net emission with annual average values of 6.67 and 1.21 ng m^{-2} h^{-1} respectively. Daily variations of GEM fluxes showed an increasing emission with the increasing air temperature and solar radiation in the daytime to a peak at 1:00 pm, and decreasing emission thereafter, even as a GEM sink or balance at night. High temperature and low air Hg concentration resulted in the high Hg emission in summer. Low temperature in winter and Hg absorption by plant in spring resulted in low Hg emission, or even adsorption in the two seasons. GEM fluxes were positively correlated with air temperature, soil temperature, wind speed, and solar radiation while negatively correlated with air humidity and atmospheric GEM concentration. The lower emission fluxes of GEM at the contaminated site (HT) when comparing with that in the clean site (QYZ), may result from a much higher adsorption fluxes at night in spite of a similar or higher emission fluxes during daytime. It testified that the higher atmospheric GEM concentration at HT restricted the forest GEM emission. Great attention should be paid on forest as a critical increasing Hg emission source with the decreasing atmospheric GEM concentration in polluted area because of the Hg emission abatement in the future.

1 Introduction

Mercury (Hg) is a world-wide concerned environmental contaminant due to its cyclic transport between air, water, soil, and the biosphere, and its tendency to bioaccumulate in the environment as neurotoxic mono-methylated compounds(CH_3Hg-) (Driscoll et al., 2013), which can cause damage to the environment and human health (Lindqvist et al., 1991). Atmospheric Hg exists in three different forms with different chemical and physical properties: gaseous elemental mercury (GEM, Hg^0), gaseous oxidized mercury (GOM, Hg^{2+}), and particulate-bound mercury (PBM, Hg^p). Because of its mild reactivity, high

31 volatility, and low dry deposition velocity and water solubility, GEM is the most abundant form of Hg in the atmosphere

32 (Gustin and Jaffe, 2010; Holmes et al., 2010), and can long-distance transport due to the long residence time (0.5~2 yr)

33 (Schroeder et al., 1998).

34 Hg emission flux from anthropogenic sources has been quantified with reasonable consistency from 1900 to 2500 t yr-1 (Streets

35 et al., 2009; Streets et al., 2011; Zhang et al., 2015; Zhang et al., 2016). However, the present estimates of natural Hg emission

36 from waters, soils, and vegetation are poorly constrained and have large uncertainties, with the values larger than anthropogenic

37 emission (e.g., 2000 t yr^{-1}, Lindqvist et al., 1991; 5207 t yr^{-1}, Pirrone et al., 2010; 4080~6950 t yr^{-1}, UNEP, 2013; 4380~6630

38 t yr^{-1} Zhu et al., 2016). The reliable quantification of natural Hg source, specifically GEM exchange between terrestrial

39 ecosystem and the atmosphere would contribute to the understanding of global and regional Hg cycling budgets (Pirrone et al.,

40 2010; Wang et al., 2014b; Song et al., 2015).

41 As a dominant ecosystem on the Earth, forest is generally regarded as an active pool of Hg (Lindberg et al., 2007; Ericksen et

42 al., 2003; Sigler et al., 2009). Hg in the forest ecosystem is derived primarily from atmospheric deposition (Grigal, 2003), and

43 foliar uptake of GEM has been recognized as a principal pathway for atmospheric Hg to enter terrestrial ecosystems (Frescholtz

44 et al., 2003; Niu et al., 2011; Obrist, 2007). Accumulated Hg in foliage is transferred to soil reservoirs via plant detritus (St

45 Louis et al., 2001) or may partially be released back into the atmosphere (Bash and Miller, 2009). In addition, Hg may enter

46 the foliage by recycling processes, releasing GEM from underlying soil surfaces (Millhollen et al., 2006b). Soil–air GEM

47 exchange is controlled by numerous factors including physicochemical properties of soil substrate and abiotic/biotic processes

48 in the soil, meteorological conditions, and atmospheric composition (Bahlmann et al., 2006; Carpi and Lindberg, 1997; Engle

49 et al., 2005; Fritsche et al., 2008a; Gustin, 2011; Rinklebe et al., 2010; Mauclair et al., 2008; Zhang et al., 2008). The majority

50 of reported GEM flux measurements over terrestrial soils indicated net emission in warmer seasons and near-zero fluxes at

51 cold temperatures (Sommar et al., 2013). There are ongoing debates regarding whether or not forest is a sink or a source of

52 GEM because the forest/air exchange flux is the sum of vegetation and soil exchange flux, depending on not only atmospheric

53 concentration and meteorological conditions, but also plant community composition (Bash and Miller, 2009; Converse et al.,

54 2010) over shorter or longer periods.

55 China is currently the world's top emitter of anthropogenic Hg with a value of 538t in 2010 (Zhang et al., 2015) and 530t in

56 2014 (Wu et al., 2016), which resulted in an elevated Hg deposition to terrestrial ecosystem and thus Hg accumulate in land

57 surface. Given the forest is likely to have large GEM re-emission of legacy Hg stored through old-deposition, it is important

58 to know the role of forests in China in global Hg transport and cycle. However, there are far fewer long-time studies of forest

59 GEM exchange flux in China, especially for the subtropical forest, which is unique in the world. In this study, directly

60 measurements of net exchange of GEM over canopy of subtropical forests was conducted at a relatively clean site and a

61 relatively polluted site impacted by an adjacent Hg mine in south China. The objective of this study is to quantify the natural

62 Hg emission from the typical forest ecosystems, and analyse its influencing factors.

63 ## 2 Materials and methods

64 ### 2.1 Site description

65 This study was conducted at Qianyanzhou (QYZ) and Huitong (HT) experimental stations managed by the Chinese Academy

66 of Sciences (CAS) and Central South University of Forestry and Technology (CSUFT), respectively. The QYZ station

67 (115º04'E, 26º45'N) is located in Taihe county, Jiangxi province (Figure1, Table 1), surrounded by farmland, with no

68 obviously anthropogenic mercury sources such as coal-fired power plants and metal smelters in 25 km around. The HT station

69 (109º45'E, 26º50'N) is located in Huitong county, Hunan province, about 100 km away from the Wanshan Mercury Mine (WS),

70 which used to be the largest mercury mine in China. The two study sites have the similar climate condition. The dominant soil

71 and vegetation types (Table 1) are widely distributed in subtropical monsoon climate zone in south China. The subtropical

72 evergreen coniferous forests have fairly thick canopy, even in winter.

73 ### 2.2 Flux monitoring

74 The continuous monitoring system of GEM vertical concentration gradient over forest canopy included a Hg detector, two

75 series of intake pipeline, and an automatically controlled valve system (Figure 2). The air sampling head and pipeline was

76 arranged on the flux tower, while the valve system and mercury detector was set in the cabin near the flux tower. Two automatic

77 GEM analyzers, model 2537X and 2537B (Tekran Instruments Inc.), with the same working principle and the detection limit

78 (less than 0.1 ng m^{-3}, Gustin et al., 2013), were used at QYZ and HT site respectively. Air intakes were placed at two different

79 heights (25 and 35 m of the 41 m-high flux tower at QYZ site; 22.5 and 30.5 m on the 33m-high flux tower at HT site).

80 Considering the extremely large disturbance of temperature and wind speed over forest canopy, especially close to the canopy,

81 the lower air intake should be set at least half canopy height (Table 1) above the canopy to ensure the stability of the results

82 (Lindberg et al., 1998). Besides, all the air intakes would be fixed out of the tower body more than 1 m to avoid the influence

83 of the tower. Passing a particulate filter membrane (0.2 μm) and a soda lime adsorption tank just after the intake to remove

84 particulate matters, organic matters and acid gases, the in-gas from each height was pumped through a separated pipe (Φ =

85 0.25 in) to the same Hg detector in turn, controlled by two 3-way electromagnetic valves manipulated by a time relay. The

86 electromagnetic valve switched once every 10 min, i.e., the measuring time of the gas from each height was 10 min, and it

87 took 20 min for a whole measuring cycle. The design of the system including the pump ensured the continuing air flow at the

88 same velocity in the two pipeline, whether the gas was sent to detect or no, to avoid the retention of air of the last cycle in the

89 pipeline. The pipeline, air intakes and valves are made of Teflon to avoid the adsorption of Hg.

90 Meteorological parameters were also measured continuously by setting air temperature, humidity and wind speed sensors at

91 the two heights (same to the air intakes), the solar radiation sensor and rainfall monitor at the higher height, and soil temperature

92 and moisture sensors at 5 cm depth in soil about 20 m away from the flux tower. All the sensors adopted international advanced

93 and reliable model (Table S1). All kinds of meteorological data were output by the data acquisition system (CR1000, Campbell

94 Scientific Inc., USA) every five minutes.

Atmospheric
Chemistry
and Physics
Discussions

95 The observations of GEM concentration gradient and meteorological parameters lasted for one year at both sites from January

96 to December in 2014.

2.3 GEM flux calculation

98 The dynamic Flux Chamber (DFCs) and micrometeorological techniques (MM) are the mostly widely applied approaches for

99 surface/atmosphere GEM flux quantification (Zhu et al., 2016). The MM methods, including of direct flux measurement

100 method (the relaxed eddy accumulation method, REA) and the gradient methods (further divided to the aerodynamic gradient

101 method, AGM, and the modified Bowen-ratio method, MBR), were usually defined to measure the GEM flux over forest

102 canopy with the advantages of no interference on measuring interface and high capability of chronical measuring large scale

103 fluxes. The AGM method, which has been used over grasslands, agricultural lands, salt marshes, landfills, and snow surface

104 (Lee et al., 2000; Kim et al., 2001; Kim et al., 2003; Cobbett et al., 2007; Cobbett and Van Heyst, 2007; Fritsche et al., 2008b;

105 Fritsche et al., 2008c; Baya and Van Heyst, 2010), was used in this study. According to the AGM method, the GEM fluxes

106 (F, ng·m^{-2}·s^{-1}) over forest canopy was calculated on the basis of the measurement of the vertical concentration gradient by

107 using the following Eq. (1):

108 $$F = K\frac{\partial c}{\partial z},\tag{1}$$

109 Where K is turbulent transfer coefficient (m^2 s^{-1}), c is GEM concentration in the atmosphere (ng m^{-3}), and z is the vertical

110 height (m). Here, the GEM concentrations difference between the two air intakes divided by the height difference was assumed

111 to be the vertical gradient of atmospheric GEM concentration. Since the automatic GEM analyser switches between two gold

112 tubes and gets a value every 5 min, the two concentrations were averaged in each 10 min (matched to the single height sampling

113 interval by adjusting the time relay) to avoid possible bias caused by different gold tubes. The GEM concentration differences

114 were calculated as the average concentrations at the higher height minus the two adjacent average concentrations at the lower

115 sampling height (all in 10 min interval). Thus, the vertical gradient of air GEM concentration can be gained every 10 min.

116 Turbulent transfer coefficient K was calculated through specific steps (Supplementary Information, SI) according to the

117 similarity theory after the measurement of the wind speed and temperature profile (Yu and Sun, 2006).

2.4 Quality control

119 In order to ensure the accuracy of the measurement results, regularly maintenance and calibration was performed to the

120 continuous monitoring system at both two sites. The particulate filter membrane on the air intake was changed once a week.

121 In addition, the soda-lime tank after the air intake and the filter membrane before the Hg analyzer was replaced monthly. The

122 automatic calibration of the internal mercury source of Tekran 2537X and Tekran 2537B and manual calibration by mercury

123 injection method were done once every 24 h and one month respectively.

Atmospheric
Chemistry
and Physics
Discussions
Open Access
EGU

124   We did blank experiments, i.e., measuring the detection limit of the concentration gradient for the monitoring systems before

125   the installation, when the air intakes were both placed indoor with stable mercury concentration. It turned out that the

126   differences of GEM concentration between the pipelines were 0.004 ± 0.017 ng m^{-3} and 0.010 ± 0.024 ng m^{-3} ($n > 60$) at QYZ

127   and HT sites, respectively. The detection limit of the concentration gradient of the system was defined as the mean of detecting

128   difference results plus one standard deviation (Fritsche et al., 2008b). Therefore, the detection limits were 0.021 ng·m^{-3} and

129   0.034 ng·m^{-3} at QYZ and HT sites, respectively. It means that there was no significant difference between the two GEM

130   concentrations at different height when the discrepancy was lower than the detection limits in the field experiments. In addition,

131   the parallelity of the two pipelines in the system was detected every month by moving the air intakes to the cabin and run

132   continuously for at least 24 h. The pipeline need clean by soaking 24 h with 15% nitric acid then cleaning with ultrapure water

133   and acetone in turn, finally drying with zero mercury gas (Zero Air Tank, Tekran Inc.), until the difference of GEM

134   concentration between the two pipelines was less than 0.02 ng m^{-3}. There was an spare pipeline system at each site to avoid

135   the pause of monitoring due to pipeline cleaning.

136   The result measured by AGM represent a mean value of regional GEM flux, i.e, footprints area of tower, which is related to

137   the measuring height and meteorological conditions (Fritsche et al., 2008b). Previous study estimated that the footprint of

138   intake at 40 m height on the flux tower was 100 - 400 m (Zhao et al., 2005). Therefore, the footprints of the intakes located at

139   different height may be similar due to the relatively uniform distribution of *pinus massoniana* or *cunninghamia lanceolata*

140   forest within 500 m around the flux towers in our research.

141   The concentrations gradient lower than the system detection limit could not be truncated in case of the overestimation of GEM

142   flux when calculating the average GEM flux in previous studies (Fritsche et al., 2008b; Converse et al., 2010). The proportion

143   of the data which had the GEM concentration gradient larger than the detection limit in this study was larger than 85%, which

144   was higher than that in the previous study on grassland (about 50%; Fritsche et al., 2008b). The reason of such high quality

145   data might be the larger height difference (10m at QYZ site and 8m at HT site, vs. 2m in the grassland study), higher GEM

146   concentration, and larger exchange surface of forest than grassland. In accordance with the inaccurate measurement by AGM

147   under the high atmospheric stability (Converse et al., 2010), especially in temperature inversion, the calculation of turbulent

148   transfer coefficient K could not converge, and the flux would be eliminated. In addition, the data would be eliminated when

149   the GEM flux exceed the range of the monthly mean ± 3 standard deviations, or during instrument failure and operation

150   instability.

151   **3 Results and discussion**

152   **3.1 Hourly and daily variations in GEM concentrations and fluxes**

153   QYZ and HT stations have both subtropical monsoon climate, with hot and rainy summers, and cold and dry winters (Table

154   S2). Atmospheric GEM concentrations were lower during spring and summer, and higher in winter and fall, with an annual

155   average value of 3.64 ng m^{-3} (1.89 ~ 6.26 ng m^{-3}, 5% ~ 95% confidence interval） at QYZ site (Figure 3), which was far higher

Atmospheric
Chemistry
and Physics
Discussions

156 than the mercury concentrations in background region in the northern hemisphere (1.5~2.0 ng·m^{-3}, Steffen et al., 2005; Kock

157 et al., 2005) and correspond to the observed results in southeast China (2.7~5.4 ng·m^{-3}, Wang et al., 2014a). Although there

158 were no major anthropogenic mercury emission sources near the QYZ station, the high concentration may be attributed to

159 regional residential coal combustion and high background GEM concentration in China. The annual average GEM

160 concentration at HT station was 5.93 ng m^{-3} (2.46 ~ 11.6 ng m^{-3}, 5% ~ 95% confidence interval）, even higher than that at QYZ

161 station, because HT station was affected by WS Mercury Mine.

162 The diurnal variation of fluxes indicated that the GEM flux increased gradually with the increase in air temperature and solar

163 radiation in the daytime in all four seasons. The peak fluxes were averaged to 30.9, 29.3, 50.9 and 29.6 ng m^{-2} h^{-1} (22.6, 46.2,

164 46.2 and 44.7 ng m^{-2} h^{-1}) in winter (December - February), spring (March - May), summer (June - August) and fall (September

165 – November) respectively at QYZ (HT) at around 1:00 pm. In contrast, the GEM fluxes were stable at around zero or even

166 negative at night, indicating a state of Hg balance at QYZ site and a strong sink at HT site. This pattern was similar to the Hg

167 emission characteristics of soil (Ma et al., 2016), vegetation (Luo et al., 2016), and terrestrial surfaces (Stamenkovic et al.,

168 2008). Modelling results of the diurnal variation of GEM fluxes over canopy for deciduous needle-leaf forest (Wang et al.,

169 2016) also showed the similar trend.

170 A clear GEM absorption (negative fluxes) not only occurred at night but also in the morning in spring at both sites (Figure 4b).

171 A small and a large depletion peaked at 9:00 am and 11:00 am at QYZ and HT sites, respectively in spring might result from

172 the vegetation uptake, which was found by direct monitoring of GEM emission from foliage (Luo et al., 2016; Converse et al.,

173 2010; Stamenkovic and Gustin, 2009). The daytime-GEM emission fluxes were significantly higher in summer and lower in

174 winter with the changes of air temperature and solar radiation. With longer daytime and higher temperature, there were fewer

175 hours per day in a state of GEM sink in summer (Figure 4c). The atmosphere-forest exchange of GEM became weaker in the

176 fall as the decline in temperature and the dormant of plant growth (Figure 4d). There were also seasonal differences on diurnal

177 variation of GEM emission from soil (Ma et al., 2016) and vegetation (Luo et al., 2016), with highest values occurring in

178 summer, followed by spring and fall, while the lowest value in winter.

179 The two stations had the similar temperature due to the same climate condition and latitude (Table 1 and S2). Relatively higher

180 value and later peak of solar radiation (except for summer) at HT site might result from the higher altitude and lower longitude,

181 which would delay the peaks of emission flux in winter, spring, and fall. Relatively larger standard variance of GEM flux at

182 HT site indicated the higher fluctuation, which might be ascribed to the fluctuating GEM concentration. HT station is close to

183 WS Mercury Mine, the GEM concentration is vulnerable to the meteorological factors like wind direction.

184 **3.2 Monthly variations in GEM concentrations and fluxes**

185 The monthly mean value of GEM concentration seemed quite even throughout the year at both QYZ and HT Sites, with three

186 peak values in January, June, and November (4.52, 4.32, and 4.25 ng m^{-3} at QYZ site; 6.73, 6.74, and 7.14 ng m^{-3} at HT site),

187 and two bottom values of 2.33and 2.89 ng m^{-3} (in March and July) at QYZ site and 4.29 and 3.34 ng m^{-3} (in February and July)

188 at HT site. In generally, monthly variations of fluxes exhibited an opposite trend of the concentration, almost all the larger

189 fluxes emerged in the months with lower GEM concentration.

190 All the monthly mean GEM fluxes were positive at QYZ station (Figure 5), indicating that the forest was net atmospheric

191 GEM source in each month. The relatively low GEM flux (3.13 ng m^{-2} h^{-1}) and lowest air temperature (7.15 °C) occurred in

192 December. The monthly mean GEM fluxes rapidly rose from December to March, coinciding with the increase in air

193 temperature and solar radiation, followed by a sudden fall to 1.56 ng m^{-2} h^{-1} in April, and a slight increase to 4.40 ng m^{-2} h^{-1} in

194 June. After that, the GEM flux rapidly increased to 11.5 ng m^{-2} h^{-1} in July and peaked at August (12.8 ng m^{-2} h^{-1}), then gradually

195 reduced to 6.84 ng m^{-2} h^{-1} in November, corresponding to the decrease in air temperature. Generally, the increase of solar

196 radiation and air temperature would cause the increasing in GEM emission from soil and vegetation. The monthly variations

197 of annual Hg emission fluxes from forest soil in South Korea showed similar trend with air temperature (Han et al., 2016).

198 Mainly affected by soil emissions, the changes of GEM fluxes showed similar trend as those of air temperature and solar

199 radiation in winter and fall. In contrast, the GEM fluxes greatly decreased in the growing season, mainly influenced by

200 vegetation uptake of GEM (Millhollen et al., 2006a; Stamenkovic and Gustin, 2009).

201 Different from QYZ station, the forest was a GEM sink in November, December and January with a negative value of monthly

202 mean GEM flux of -6.82, -7.64, and -3.60 ng m^{-2} h^{-1} respectively at HT station (Figure 5). The monthly mean GEM fluxes

203 gradually elevated and became positive in February to April, subsequently fell to negative in May. Then, coinciding with the

204 change of air temperature, the GEM fluxes increased again, peaked in August (6.86 ng m^{-2} h^{-1}), and gradually decreased to

205 negative in November. Although monthly variation of GEM fluxes at HT site was similar to that at QYZ site, HT site had

206 overall lower GEM fluxes but higher atmospheric GEM concentration than QYZ station. The annual average atmospheric

207 mercury concentration at HT site was 62% higher than that at QYZ site (Table 1). Higher concentrations of atmospheric

208 mercury would inhibit the Hg release from soil and plants, and increase the GEM absorption of foliage (see also in section

209 3.2). In addition to the influence of high atmospheric GEM concentration, the current-year foliage of *cunninghamia lanceolata*

210 (dominant species at HT station, Table 1) have larger absorption than *pinus massoniana* at QYZ indicated by larger Hg content

211 in needles and litters (Figure S1; Luo et al., 2016).

212 The monthly mean daytime-GEM fluxes always had positive values, which were much larger than the values at night (with

213 small negative values in December, January, April and May, and near-zero in other months) at QYZ site (Figure 6). Thus, the

214 GEM flux over forest canopy was mainly attributed to the emission during the daytime at QYZ site. The monthly mean GEM

215 fluxes were also positive during the daytime but all negative at night at HT site. HT site had larger monthly mean emission

216 fluxes during the daytime and larger absorption fluxes at night (Figure 6). As a total effect, the monthly fluxes were lower than

217 those in QYZ (Figure 5).

218 **3.3 Factors influencing GEM flux**

219 In order to evaluate the influences of the environmental conditions and atmospheric GEM concentration on the GEM fluxes,

220 the correlation analysis between the flux and each factor had been calculated (Table 2). It showed that the GEM flux over

Atmospheric
Chemistry
and Physics
Discussions

221 forest canopy was negatively correlated with atmospheric GEM concentration at both sites except in summer at QYZ station.

222 The inhibiting effect of atmospheric GEM concentration on GEM emission was not only reflected by the lower emission fluxes

223 at HT site comparing with those in QYZ site (Figure 5), but also by an instant decline in GEM flux after a sudden increase in

224 ambient GEM concentration. For instance, continuous measurement data during five typical days in each season (Figure 7)

225 showed an absorption peak on February 3 and May 5 at QYZ site and February 20, May 14 and August 23 at HT site caused

226 by the increase in air GEM concentrations. According to the wind direction records, the sudden rise of GEM concentration to

227 22.94 ng·m^{-3} on May 14 at HT site might be caused by the approach of a high-mercury-content air mass from WS Mercury

228 Mine leading by northwest wind. Elevated ambient GEM concentration has been found to suppress GEM flux by reducing the

229 GEM concentration gradient at the interfacial surfaces (Xin and Gustin, 2007). At locations where ambient Hg concentration

230 is high, absorption (or deposition) is predominately observed despite of influence of meteorological factors (Wang et al., 2007;

231 Niu et al., 2011). Although the increase in GEM concentration would inhibit mercury emissions of foliage and soil, the

232 emission fluxes had positive correlation with atmospheric GEM concentration in summer (Figure S2) because the large

233 emission of GEM concentration in hot summer might result in an increase of air mercury concentration.

234 The GEM flux was positively correlated with solar radiation, air temperature, and wind speed at both QYZ and HT sites (Table

235 2). Solar radiation has been found to be highly positively correlated with soil and vegetation GEM flux (Carpi and Lindberg,

236 1997; Boudala et al., 2000; Zhang et al., 2001; Gustin et al., 2002; Poissant et al., 2004; Bahlmann et al., 2006), because it can

237 enhance Hg^{2+} reduction and therefore facilitate GEM evasion (Gustin et al., 2002). For instance, there was a high GEM

238 emission peak at noon in winter (Figure 7; from February 1 to 3 at QYZ site and February 19 to 20 at HT site) even with

239 extremely low temperature. In addition to solar radiation, air temperature had significant effect on GEM flux, especially in

240 summer. Continued GEM emissions occurred in the daytime without strong solar radiation, or in the evening under the high

241 temperature in the summer (Figure 7; August 18 to 19 at QYZ site). Recent studies also showed that the GEM emission flux

242 from soil would be mainly controlled by the air temperature (Moore and Carpi, 2005; Bahlmann et al., 2006). Compared with

243 that in summer, GEM emission peak had decreased (Figure 7; 53.0 and 60.8 ng·m^{-3} h^{-1} on November 9 and 10 vs. 77.6 on

244 August 16 at QYZ site; 213, 206 and 103 ng·m^{-3} h^{-1} on November 15, 16 and 18 vs. 322 and 276 ng·m^{-3} h^{-1} on August 21 and

245 22 9 in HT site) on the sunny day in the fall due to the decrease in temperature. In addition, as wind speed increased, the air

246 turbulence on the surface of soil and foliage would speed up, and thus enhance the desorption of GEM on the interface

247 (Wallschlager et al., 2002; Gillis and Miller, 2000; Eckley et al., 2010; Lin et al., 2012), which may explain the positive

248 correlation between GEM flux and wind speed. Soil temperature mainly impacting on the emission of soil, and also showed

249 positive correlation with GEM fluxes except for in the winter with low soil temperature (Table 2). One possible explanation

250 of the exception was that the change of soil temperature had no significant influence on the microbial activity and the reaction

251 rate in soil if soil temperature was lower than a certain value (Corbett-Hains et al., 2012).

252 Air humidity generally was negatively correlated to the GEM flux over forest canopy (Table 2). Higher relative humidity may

253 decrease stomatal conductance and thus lower transpiration of needles, which would result in decreases in GEM emissions

254 (Luo et al., 2016). The correlation between GEM flux and soil moisture was not sure at QYZ station, e.g., positive in winter,

Atmospheric
Chemistry
and Physics
Discussions

255 negative in spring and fall, but no significance in summer. It seems that the influence of soil moisture on soil mercury emissions

256 was uncertain, depends on the state soil water saturation (Figure S3). Previous studies supported that adding water to dry soil

257 promotes Hg reduction, because water molecules likely replace soil GEM binding sites and facilitates GEM emission. However,

258 Hg emission is suppressed in water saturated soil because the soil pore space filled with water hampers Hg mass transfer (Gillis

259 and Miller, 2000; Gustin and Stamenkovic, 2005; Pannu et al., 2014). For instance, intensive soil GEM emission was

260 synchronized to the rainfall at around 9:00 pm on August 16 and 8:00 pm on August 17 at QYZ site (Figure 7). In addition,

261 the continuous but weaker rainfall from November 6 to 7 might also increase the GEM emission, in comparison with that in

262 November 8 under the same solar radiation and temperature. Actually, continuous but weaker rainfall would lead to the

263 increase of soil moisture, but not necessarily caused soil water saturation. Soil moisture content monitoring results had shown

264 that the soil moisture content had a certain rise but remained below 0.28 during this period, which was lower than the highest

265 value (0.52) during the annual monitoring. However, no significant emission flux was observed on August 19 after a series of

266 strong rainfall. Repeated rewetting experiments showed a smaller increase in emission, implying GEM needs to be resupplied

267 by means of reduction and dry deposition after a wetting event (Gustin and Stamenkovic, 2005; Song and Van Heyst, 2005;

268 Eckley et al., 2011). The correlation between GEM flux and soil moisture was not significant in all of the seasons since the

269 fluctuation of soil moisture content was small with the annual range of 0.21~0.34 at HT site, and the change of soil moisture

270 content had far less impact on the soil GEM emissions.

271 The temporal variation of vegetation growth would play an important role in the forest GEM emission because of the vital

272 function of vegetation to Hg cycle in forest ecosystem through changing environmental variables at ground surfaces (e.g.,

273 reducing solar radiation, temperature and friction velocity) (Gustin et al., 2004), and providing active surfaces for Hg uptake.

274 Recent measurements suggested that air–surface exchange of GEM is largely bidirectional between air and plant, and that

275 growing plants act as a net sink (Ericksen et al., 2003; Stamenkovic et al., 2008; Hartman et al., 2009). The negative exchange

276 GEM fluxes at night at both two sites in this study should be mainly attributed to GEM adsorption by vegetation (Figure 6).

277 In addition, GEM absorption capacity of foliage began to weaken at the end of growing season in November when the

278 absorption peaks were smaller than that in spring at both QYZ and HT sites (Figure 7). The stomata open in the morning will

279 also accelerate the forest absorption of Hg by vegetation, lead to the emergence of absorption peak even in the morning (Luo

280 et al., 2016).

281 **3.4 Forest as source/sink of GEM**

282 GEM flux measurements over forest canopy indicated that QYZ forest at the clean site was a net source of GEM in all seasons,

283 with the highest and lowest GEM emissions in summer (8.09 ng m^{-2} h^{-1}) and spring (5.25 ng m^{-2} h^{-1}, early growing season)

284 respectively. In contact, significant differences in GEM fluxes were observed among seasons at HT, the contaminated site,

285 indicating a clear sink in winter (dormant season), a slight source in spring and fall, and a large source in summer (Table 3).

286 As the total effect, the forest ecosystem at HT site had a net GEM emission with a magnitude of 1.21 ng m^{-2} h^{-1} for a whole

287 year. These results suggest that the subtropical forests in our study region should be the substantial GEM source, and the

Atmospheric
Chemistry
and Physics
Discussions

288   differences among seasons emphasized the importance of capturing GEM flux seasonality when determining total Hg budgets.

289   As mentioned before, there was almost no difference of climate conditions between QYZ and HT sites, with the similar soil

290   type and latitude, and little difference in the vegetation growth. However, the HT site with higher atmospheric GEM

291   concentration had relatively lower GEM fluxes in all seasons in comparison with those in QYZ site. It emphasized again the

292   importance of atmospheric GEM concentration on the GEM fluxes.

293   The GEM fluxes over forest canopy were the sum of emission fluxes from soil and vegetation, and extremely difficult to

294   quantify. GEM exchange of foliage/atmosphere or soil/atmosphere is both bi-directional, with net adsorption occurring at

295   elevated air Hg concentration while net emission when typical ambient concentration was lower than the "compensation point"

296   (Converse et al., 2010; Ericksen et al., 2003; Stamenkovic et al., 2008; Hartman et al., 2009). However, the study of

297   foliage/atmosphere mercury exchange at QYZ indicated that the vegetation presented as a net GEM source in all seasons, but

298   a clear sink in the growing season with stomatal opening (Luo et al., 2016) even under the relatively lower atmospheric GEM

299   concentration. Until now, there are merely few researches using AGM to monitor the GEM flux above forest canopy even in

300   short period. Previous studies showed that the exchange fluxes of GEM vary in sign and magnitude (Table 3). Lindberg et al.

301   (1998) measured GEM fluxes over a mature deciduous forest, a yang pine plantation, and a boreal forest floor using the MBR

302   method and suggested that global forest is a net source of GEM with an emission of 10-330, 17-86 and 1-4 ng m^{-2} h^{-1} at daytime,

303   respectively (Table 3). The observation of Hg fluxes in a deciduous forest using a REA method showed a net GEM emission

304   of 21.9 ng m^{-2} h^{-1} during summer (Bash and Miller, 2008). However, a study in Québec, Canada showed that GEM

305   concentrations at a maple forest site are consistently lower than those measured at an adjacent open site, indicating a Hg sink

306   for the forest (Poissant et al., 2008). Similarly, the lower GEM concentrations observed in leaf-growing season at forest sites

307   across the Atmospheric Mercury Network (AMNet) in USA (Lan et al., 2012), Coventry Connecticut, England (Bash and

308   Miller, 2009), Mt. Changbai, Northeast China (Fu et al., 2016) also suggest forest as a net GEM sink during the growing season.

309   Different results were obtained by AGM and MBR method at the same time (Converse et al., 2010) (Table 3). There was

310   limiting comparability of fluxes data reported in literature because of the lack of a standard method protocol for GEM flux

311   quantification (Gustin, 2011; Zhu et al., 2015). Although the discrepancy in the measured GEM exchanges between forest and

312   atmosphere is partially attributed to the uncertainties of the flux quantification method (Sommar et al., 2013), forest structure,

313   climate condition, background Hg concentration, and forest soil Hg content could play critical roles in GEM emission from

314   forest ecosystem. Unlike deciduous forest as a sink of GEM in most previous studies, the evergreen foliage in the subtropical

315   forests in this study (in spite of the seasonal variations of vegetation growth) was demonstrated as a net GEM source to the

316   atmosphere (Luo et al., 2016). In addition, extremely high soil Hg content (42.6 and 167 ng g^{-1} at QYZ and HT sites shown in

317   Table 1, while 63 ng g^{-1} in in Québec, Canada; Poissant et al., 2008) result from long-term elevated Hg deposition, the high

318   temperature and solar radiation would contribute the net emission flux of GEM from both forest soil and vegetation in

319   subtropical, south China. However, the observations in this study were not higher than the results in the forests as GEM sources

320   in previous studies, possibly due to the higher ambient GEM concentration (3.64 and 5.93 ng m^{-3} at QYZ and HT sites vs.

321   2.23 ng m^{-3} in Tennessee, USA and 1.34 in Connecticut, USA; Table 3).

Atmospheric
Chemistry
and Physics
Discussions

4 Conclusions and implication

The high quality direct observation data of a clean and a contaminated site with typical climate, vegetation type and soil type in south China could be important for implications for the regional Hg cycling estimation, and the awareness of the role of forests in the global mercury cycle. From continuously quantitative MM-flux measurements covering wide temporal scales at QYZ and HT sites in subtropical south China, it is inferred that forest ecosystems can represent a net GEM source with the average magnitudes of 6.67 and 1.21 ng m^{-2} h^{-1} for a full year at a clean site (QYZ) and a contaminated site (HT), respectively. GEM flux measurements were net source in all seasons at the clean site, with the highest in summer because of the relatively high air temperature and radiation, and lowest in spring result from the vegetation growth. For the contaminated site, a net sink occurred in the winter, a significant source in summer, and no significant flux during spring and fall. The GEM emission dominated in the daytime, and peaked at around 1:00 pm, while the forest served as a GEM sink or balance at night. It is worth noting that there was a lower emission fluxes of GEM at the contaminated site result from similar or even higher emission fluxes during daytime, but much higher adsorption fluxes at night than the clean site under the similar meteorological conditions. Although, the larger Hg content in soil would enhance the emission of soil and vegetation, the elevated GEM concentration suppresses the Hg emission, and increase the absorption by vegetation at the contaminated site. The result indicated that the atmospheric GEM concentration play an importance role in inhibiting the GEM fluxes between forest and air, coinciding with the negative correlation between GEM fluxes and atmospheric GEM concentration. In addition, the forest should be pay attention as a critical increasing source with the decline atmospheric GEM concentration because the Hg emission abatement in the future, and the increasing emission might result from the re-emission of legacy Hg stored in the forest.

The GEM flux over forest canopy was the sum emission flux of soil and vegetation, and showed monthly variations caused by the temporal variation of vegetation growth, atmospheric GEM concentration and meteorological conditions including of air temperature, radiation and wind speed. The correlation between GEM fluxes and factors had been analysed, combined with the characteristics of GEM exchange between soil (or foliage) and air. It indicated that GEM fluxes were positively correlated with air temperature, soil temperature, wind speed, and solar radiation, but negatively correlated with air humidity. The influence of soil moisture content was uncertain, depends on whether the soil water saturated and the initial state of the soil. In addition, vegetation growth would play an important role in the decline in forest GEM emission in spring. The difference in climate conditions and ambient GEM concentration should be considered when estimating the global forest GEM emission.

References

354

355 Bahlmann, E., Ebinghaus, R., and Ruck, W.: Development and application of a laboratory flux measurement system (LFMS)
356   for the investigation of the kinetics of mercury emissions from soils, Journal of Environmental Management, 81, 114-
357   125, 10.1016/j.jenvman.2005.09.022, 2006.

358 Bash, J. O., and Miller, D. R.: A relaxed eddy accumulation system for measuring surface fluxes of total gaseous mercury,
359   Journal of Atmospheric and Oceanic Technology, 25, 244-257, 10.1175/2007jtecha908.1, 2008.

360 Bash, J. O., and Miller, D. R.: Growing season total gaseous mercury (TGM) flux measurements over an Acer rubrum L. stand,
361   Atmos. Environ., 43, 5953-5961, 10.1016/j.atmosenv.2009.08.008, 2009.

362 Baya, A. P., and Van Heyst, B.: Assessing the trends and effects of environmental parameters on the behaviour of mercury in
363   the lower atmosphere over cropped land over four seasons, Atmos. Chem. Phys., 10, 8617-8628, 10.5194/acp-10-8617-
364   2010, 2010.

365 Boudala, F. S., Folkins, I., Beauchamp, S., Tordon, R., Neima, J., and Johnson, B.: Mercury flux measurements over air and
366   water in Kejimkujik National Park, Nova Scotia, Water Air Soil Pollut., 122, 183-202, 10.1023/a:1005299411107, 2000.

367 Carpi, A., and Lindberg, S. E.: Sunlight-mediated emission of elemental mercury from soil amended with municipal sewage
368   sludge, Environ. Sci. Technol., 31, 2085-2091, 10.1021/es960910+, 1997.

369 CAS., C., (The China Vegetation Editiorial Committee, Chinese Academy of Science): Vegetation map of the People's
370   Republic of China (1:1000 000), 2007. (In Chinese)

371 Cobbett, F. D., Steffen, A., Lawson, G., and Van Heyst, B. J.: GEM fluxes and atmospheric mercury concentrations (GEM,
372   RGM and Hg-P) in the Canadian Arctic at Alert, Nunavut, Canada (February-June 2005), Atmos. Environ., 41, 6527-
373   6543, 10.1016/j.atmonsenv.2007.04.033, 2007.

374 Cobbett, F. D., and Van Heyst, B. J.: Measurements of GEM fluxes and atmospheric mercury concentrations (GEM, RGM
375   and Hg-P) from an agricultural field amended with biosolids in Southern Ont., Canada (October 2004-November 2004),
376   Atmos. Environ., 41, 2270-2282, 10.1016/j.atmosenv.2006.11.011, 2007.

377 Converse, A. D., Riscassi, A. L., and Scanlon, T. M.: Seasonal variability in gaseous mercury fluxes measured in a high-
378   elevation meadow, Atmos. Environ., 44, 2176-2185, 10.1016/j.atmosenv.2010.03.024, 2010.

379 Corbett-Hains, H., Walters, N. E., and Van Heyst, B. J.: Evaluating the effects of sub-zero temperature cycling on mercury
380   flux from soils, Atmos. Environ., 63, 102-108, 10.1016/j.atmosenv.2012.09.047, 2012.

381 Driscoll, C. T., Mason, R. P., Chan, H. M., Jacob, D., and Pirrone, N.: Mercury as a global pollutant: sources, pathways and
382   effects, Environ. Sci. Technol., 47, 4967-4983, 2013.

383 Eckley, C. S., Gustin, M., Lin, C. J., Li, X., and Miller, M. B.: The influence of dynamic chamber design and operating
384   parameters on calculated surface-to-air mercury fluxes, Atmos. Environ., 44, 194-203, 10.1016/j.atmosenv.2009.10.013,
385   2010.

Atmospheric Chemistry and Physics Discussions / EGU Open Access

386 Eckley, C. S., Gustin, M., Miller, M. B., and Marsik, F.: Scaling non-point-source mercury emissions from two active industrial
387   gold mines: influential variables and annual emission estimates, Environ. Sci. Technol., 45, 392-399, 10.1021/es101820q,
388   2011.

389 Engle, M. A., Gustin, M. S., Lindberg, S. E., Gertler, A. W., and Ariya, P. A.: The influence of ozone on atmospheric emissions
390   of gaseous elemental mercury and reactive gaseous mercury from substrates, Atmos. Environ., 39, 7506-7517,
391   10.1016/j.atmosenv.2005.07.069, 2005.

392 Ericksen, J. A., Gustin, M. S., Schorran, D. E., Johnson, D. W., Lindberg, S. E., and Coleman, J. S.: Accumulation of
393   atmospheric mercury in forest foliage, Atmos. Environ., 37, 1613-1622, 10.1016/s1352-2310(03)00008-6, 2003.

394 Frescholtz, T. F., Gustin, M. S., Schorran, D. E., and Fernandez, G. C. J.: Assessing the source of mercury in foliar tissue of
395   quaking aspen, Environmental Toxicology and Chemistry, 22, 2114-2119, 10.1897/1551-
396   5028(2003)022<2114:atsomi>2.0.co;2, 2003.

397 Fritsche, J., Obrist, D., and Alewell, C.: Evidence of microbial control of Hg^0 emissions from uncontaminated terrestrial soils,
398   Journal of Plant Nutrition and Soil Science-Zeitschrift Fur Pflanzenernahrung Und Bodenkunde, 171, 200-209,
399   10.1002/jpln.200625211, 2008a.

400 Fritsche, J., Obrist, D., Zeeman, M. J., Conen, F., Eugster, W., and Alewell, C.: Elemental mercury fluxes over a sub-alpine
401   grassland determined with two micrometeorological methods, Atmos. Environ., 42, 2922-2933,
402   10.1016/j.atmosenv.2007.12.055, 2008b.

403 Fritsche, J., Wohlfahrt, G., Ammann, C., Zeeman, M., Hammerle, A., Obrist, D., and Alewell, C.: Summertime elemental
404   mercury exchange of temperate grasslands on an ecosystem-scale, Atmos. Chem. Phys., 8, 7709-7722, 2008c.

405 Fu, X., Zhu, W., Zhang, H., Sommar, J., Yu, B., Yang, X., Wang, X., Lin, C.-J., and Feng, X.: Depletion of atmospheric
406   gaseous elemental mercury by plant uptake at Mt. Changbai, Northeast China, Atmos. Chem. Phys., 16, 12861-12873,
407   10.5194/acp-16-12861-2016, 2016.

408 Gao, Y., He, N., Yu, G., Chen, W., and Wang, Q.: Long-term effects of different land use types on C, N, and P stoichiometry
409   and storage in subtropical ecosystems: A case study in China, Ecological Engineering, 67, 171-181, 2014.

410 Gillis, A. A., and Miller, D. R.: Some local environmental effects on mercury emission and absorption at a soil surface, Sci.
411   Total Environ., 260, 191-200, 10.1016/s0048-9697(00)00563-5, 2000.

412 Grigal, D. F.: Mercury sequestration in forests and peatlands: A review, Journal of Environmental Quality, 32, 393-405, 2003.

413 Gustin, M., and Jaffe, D.: Reducing the uncertainty in measurement and understanding of mercury in the atmosphere, Environ.
414   Sci. Technol., 44, 2222-2227, 10.1021/es902736k, 2010.

415 Gustin, M. S., Biester, H., and Kim, C. S.: Investigation of the light-enhanced emission of mercury from naturally enriched
416   substrates, Atmos. Environ., 36, 3241-3254, 10.1016/s1352-2310(02)00329-1, 2002.

417 Gustin, M. S., Ericksen, J. A., Schorran, D. E., Johnson, D. W., Lindberg, S. E., and Coleman, J. S.: Application of controlled
418   mesocosms for understanding mercury air-soil-plant exchange, Environ. Sci. Technol., 38, 6044-6050,
419   10.1021/es0487933, 2004.

Atmospheric
Chemistry
and Physics
Discussions

420   Gustin, M. S., and Stamenkovic, J.: Effect of watering and soil moisture on mercury emissions from soils, Biogeochemistry,
421   76, 215-232, 10.1007/s10533-005-4566-8, 2005.

422   Gustin, M. S.: Exchange of mercury between the atmosphere and terrestrial ecosystems, 423-451 pp., 2011.

423   Han, J.-S., Seo, Y.-S., Kim, M.-K., Holsen, T. M., and Yi, S.-M.: Total atmospheric mercury deposition in forested areas in
424   South Korea, Atmos. Chem. Phys., 16, 7653-7662, 10.5194/acp-16-7653-2016, 2016.

425   Hartman, J. S., Weisberg, P. J., Pillai, R., Ericksen, J. A., Kuiken, T., Lindberg, S. E., Zhang, H., Rytuba, J. J., and Gustin, M.
426   S.: Application of a Rule-Based Model to estimate mercury exchange for three background biomes in the Continental
427   United States, Environ. Sci. Technol., 43, 4989-4994, 10.1021/es900075q, 2009.

428   Holmes, C. D., Jacob, D. J., Corbitt, E. S., Mao, J., Yang, X., Talbot, R., and Slemr, F.: Global atmospheric model for mercury
429   including oxidation by bromine atoms, Atmos. Chem. Phys., 10, 12037-12057, 10.5194/acp-10-12037-2010, 2010.

430   Kim, K. H., Kim, M. Y., and Lee, G.: The soil-air exchange characteristics of total gaseous mercury from a large-scale
431   municipal landfill area, Atmos. Environ., 35, 3475-3493, 10.1016/s1352-2310(01)00095-4, 2001.

432   Kim, K. H., Kim, M. Y., Kim, J., and Lee, G.: Effects of changes in environmental conditions on atmospheric mercury
433   exchange: Comparative analysis from a rice paddy field during the two spring periods of 2001 and 2002, Journal of
434   Geophysical Research-Atmospheres, 108, 10.1029/2003jd003375, 2003.

435   Kock, H. H., Bieber, E., Ebinghaus, R., Spain, T. G., and Thees, B.: Comparison of long-term trends and seasonal variations
436   of atmospheric mercury concentrations at the two European coastal monitoring stations Mace Head, Ireland, and Zingst,
437   Germany, Atmos. Environ., 39, 7549-7556, 10.1016/j.atmosenv.2005.02.059, 2005.

438   Lan, X., Talbot, R., Castro, M., Perry, K., and Luke, W.: Seasonal and diurnal variations of atmospheric mercury across the
439   US determined from AMNet monitoring data, Atmos. Chem. Phys., 12, 10569-10582, 10.5194/acp-12-10569-2012, 2012.

440   Lee, X., Benoit, G., and Hu, X. Z.: Total gaseous mercury concentration and flux over a coastal saltmarsh vegetation in
441   Connecticut, USA, Atmos. Environ., 34, 4205-4213, 10.1016/s1352-2310(99)00487-2, 2000.

442   Lin, C.-J., Zhu, W., Li, X., Feng, X., Sommar, J., and Shang, L.: Novel dynamic flux chamber for measuring air-surface
443   exchange of Hg^0 from soils, Environ. Sci. Technol., 46, 8910-8920, 10.1021/es3012386, 2012.

444   Lindberg, S., Bullock, R., Ebinghaus, R., Engstrom, D., Feng, X., Fitzgerald, W., Pirrone, N., Prestbo, E., and Seigneur, C.: A
445   synthesis of progress and uncertainties in attributing the sources of mercury in deposition, Ambio, 36, 19-32, 2007.

446   Lindberg, S. E., Hanson, P. J., Meyers, T. P., and Kim, K. H.: Air/surface exchange of mercury vapor over forests - The need
447   for a reassessment of continental biogenic emissions, Atmos. Environ., 32, 895-908, 10.1016/s1352-2310(97)00173-8,
448   1998.

449   Lindqvist, Johansson, Aastrup, Andersson, Bringmark, Hovsenius, Håkanson, Iverfeldt, Meili, and Timm: Mercury in the
450   Swedish environment, Water Air & Soil Pollution, 55, 1-261, 1991.

451   Luo, Y., Duan, L., Driscoll, C. T., Xu, G., Shao, M., Taylor, M., Wang, S., and Hao, J.: Foliage/atmosphere exchange of
452   mercury in a subtropical coniferous forest in south China, J. Geophys. Res.-Biogeosci., 121, 2006-2016,
453   10.1002/2016jg003388, 2016.

454 Ma, M., Wang, D., Du, H., Sun, T., Zhao, Z., Wang, Y., and Wei, S.: Mercury dynamics and mass balance in a subtropical
455   forest, southwestern China, Atmos. Chem. Phys., 16, 4529-4537, 10.5194/acp-16-4529-2016, 2016.

456 Mauclair, C., Layshock, J., and Carpi, A.: Quantifying the effect of humic matter on the emission of mercury from artificial
457   soil surfaces, Appl. Geochem., 23, 594-601, 10.1016/j.apgeochem.2007.12.017, 2008.

458 Millhollen, A. G., Gustin, M. S., and Obrist, D.: Foliar mercury accumulation and exchange for three tree species, Environ.
459   Sci. Technol., 40, 6001-6006, 10.1021/es0609194, 2006a.

460 Millhollen, A. G., Obrist, D., and Gustin, M. S.: Mercury accumulation in grass and forb species as a function of atmospheric
461   carbon dioxide concentrations and mercury exposures in air and soil, Chemosphere, 65, 889-897,
462   10.1016/j.chemosphere.2006.03.008, 2006b.

463 Moore, C., and Carpi, A.: Mechanisms of the emission of mercury from soil: role of UV radiation, Journal of Geophysical
464   Research-Part D-Atmospheres, 110, 9 pp.-9 pp., 10.1029/2004jd005567, 2005.

465 Niu, Z., Zhang, X., Wang, Z., and Ci, Z.: Field controlled experiments of mercury accumulation in crops from air and soil,
466   Environ. Pollut., 159, 2684-2689, 10.1016/j.envpol.2011.05.029, 2011.

467 Obrist, D.: Atmospheric mercury pollution due to losses of terrestrial carbon pools?, Biogeochemistry, 85, 119-123,
468   10.1007/s10533-007-9108-0, 2007.

469 Pannu, R., Siciliano, S. D., and O'Driscoll, N. J.: Quantifying the effects of soil temperature, moisture and sterilization on
470   elemental mercury formation in boreal soils, Environ. Pollut., 193, 138-146, 10.1016/j.envpol.2014.06.023, 2014.

471 Pirrone, N., Cinnirella, S., Feng, X., Finkelman, R. B., Friedli, H. R., Leaner, J., Mason, R., Mukherjee, A. B., Stracher, G. B.,
472   Streets, D. G., and Telmer, K.: Global mercury emissions to the atmosphere from anthropogenic and natural sources,
473   Atmos. Chem. Phys., 10, 5951-5964, 10.5194/acp-10-5951-2010, 2010.

474 Poissant, L., Pilote, M., Constant, P., Beauvais, C., Zhang, H. H., and Xu, X. H.: Mercury gas exchanges over selected bare
475   soil and flooded sites in the bay St. Francois wetlands (Quebec, Canada), Atmos. Environ., 38, 4205-4214,
476   10.1016/j.atmosenv.2004.03.068, 2004.

477 Poissant, L., Pilote, M., Yumvihoze, E., and Lean, D.: Mercury concentrations and foliage/atmosphere fluxes in a maple forest
478   ecosystem in Quebec, Canada, Journal of Geophysical Research-Atmospheres, 113, 10.1029/2007jd009510, 2008.

479 Rinklebe, J., During, A., Overesch, M., Du Laing, G., Wennrich, R., Staerk, H.-J., and Mothes, S.: Dynamics of mercury fluxes
480   and their controlling factors in large Hg-polluted floodplain areas, Environ. Pollut., 158, 308-318,
481   10.1016/j.envpol.2009.07.001, 2010.

482 Schroeder, W. H., Anlauf, K. G., Barrie, L. A., Lu, J. Y., Steffen, A., Schneeberger, D. R., and Berg, T.: Arctic springtime
483   depletion of mercury, Nature, 394, 331-332, 10.1038/28530, 1998.

484 Sigler, J. M., Mao, H., and Talbot, R.: Gaseous elemental and reactive mercury in Southern New Hampshire, Atmos. Chem.
485   Phys., 9, 1929-1942, 2009.

486   Sommar, J., Zhu, W., Lin, C.-J., and Feng, X.: Field Approaches to measure Hg exchange between natural surfaces and the
487   atmosphere a review, Critical Reviews in Environmental Science and Technology, 43, 1657-1739,
488   10.1080/10643389.2012.671733, 2013.

489   Song, S., Selin, N. E., Soerensen, A. L., Angot, H., Artz, R., Brooks, S., Brunke, E. G., Conley, G., Dommergue, A., Ebinghaus,
490   R., Holsen, T. M., Jaffe, D. A., Kang, S., Kelley, P., Luke, W. T., Magand, O., Marumoto, K., Pfaffhuber, K. A., Ren, X.,
491   Sheu, G. R., Slemr, F., Warneke, T., Weigelt, A., Weiss-Penzias, P., Wip, D. C., and Zhang, Q.: Top-down constraints
492   on atmospheric mercury emissions and implications for global biogeochemical cycling, Atmos. Chem. Phys., 15, 7103-
493   7125, 10.5194/acp-15-7103-2015, 2015.

494   Song, X. X., and Van Heyst, B.: Volatilization of mercury from soils in response to simulated precipitation, Atmos. Environ.,
495   39, 7494-7505, 10.1016/j.atmosenv.2005.07.064, 2005.

496   St Louis, V. L., Rudd, J. W. M., Kelly, C. A., Hall, B. D., Rolfhus, K. R., Scott, K. J., Lindberg, S. E., and Dong, W.:
497   Importance of the forest canopy to fluxes of methyl mercury and total mercury to boreal ecosystems, Environ. Sci.
498   Technol., 35, 3089-3098, 10.1021/es001924p, 2001.

499   Stamenkovic, J., Gustin, M. S., Arnone, J. A., III, Johnson, D. W., Larsen, J. D., and Verburg, P. S. J.: Atmospheric mercury
500   exchange with a tallgrass prairie ecosystem housed in mesocosms, Sci. Total Environ., 406, 227-238,
501   10.1016/j.scitotenv.2008.07.047, 2008.

502   Stamenkovic, J., and Gustin, M. S.: Nonstomatal versus stomatal uptake of atmospheric mercury, Environ. Sci. Technol., 43,
503   1367-1372, 10.1021/es801583a, 2009.

504   Steffen, A., Schroeder, W., Macdonald, R., Poissant, L., and Konoplev, A.: Mercury in the Arctic atmosphere: An analysis of
505   eight years of measurements of GEM at Alert (Canada) and a comparison with observations at Amderma (Russia) and
506   Kuujjuarapik (Canada), Sci. Total Environ., 342, 185-198, 10.1016/j.scitotenv.2004.12.048, 2005.

507   Streets, D. G., Zhang, Q., and Wu, Y.: Projections of Global Mercury Emissions in 2050, Environ. Sci. Technol., 43, 2983-
508   2988, 10.1021/es802474j, 2009.

509   Streets, D. G., Devane, M. K., Lu, Z., Bond, T. C., Sunderland, E. M., and Jacob, D. J.: All-Time releases of mercury to the
510   atmosphere from human activities, Environ. Sci. Technol., 45, 10485-10491, 10.1021/es202765m, 2011.

511   UNEP Minamata Convention on Mercury: available at: http://www.mercuryconvention.org (last access: 25 March 2017), 2013.

512   Wallschlager, D., Kock, H. H., Schroeder, W. H., Lindberg, S. E., Ebinghaus, R., and Wilken, R. D.: Estimating gaseous
513   mercury emissions from contaminated floodplain soils to the atmosphere with simple field measurement techniques,
514   Water Air Soil Pollut., 135, 39-54, 10.1023/a:1014711831589, 2002.

515   Wang, L., Wang, S., Zhang, L., Wang, Y., Zhang, Y., Nielsen, C., McElroy, M. B., and Hao, J.: Source apportionment of
516   atmospheric mercury pollution in China using the GEOS-Chem model, Environ. Pollut., 190, 166-175,
517   10.1016/j.envpol.2014.03.011, 2014a.

518   Wang, Q., Wang, S., and Zhang, J.: Assessing the effects of vegetation types on carbon storage fifteen years after reforestation
519   on a Chinese fir site, For. Ecol. Manage., 258, 1437-1441, 10.1016/j.foreco.2009.06.050, 2009.

520 Wang, S., Feng, X., Qiu, G., Fu, X., and Wei, Z.: Characteristics of mercury exchange flux between soil and air in the heavily
521   air-polluted area, eastern Guizhou, China, Atmos. Environ., 41, 5584-5594, 10.1016/j.atmosenv.2007.03.002, 2007.

522 Wang, X., Lin, C. J., and Feng, X.: Sensitivity analysis of an updated bidirectional air-surface exchange model for elemental
523   mercury vapor, Atmos. Chem. Phys., 14, 6273-6287, 10.5194/acp-14-6273-2014, 2014b.

524 Wang, X., Lin, C.-J., Yuan, W., Sommar, J., Zhu, W., and Feng, X.: Emission-dominated gas exchange of elemental mercury
525   vapor over natural surfaces in China, Atmos. Chem. Phys., 16, 11125-11143, 10.5194/acp-16-11125-2016, 2016.

526 Wu, Q., Wang, S., Li, G., Liang, S., Lin, C.-J., Wang, Y., Cai, S., Liu, K., and Hao, J.: Temporal Trend and Spatial Distribution
527   of Speciated Atmospheric Mercury Emissions in China During 1978-2014, Environ. Sci. Technol., 50, 13428-13435,
528   10.1021/acs.est.6b04308, 2016.

529 Xin, M., and Gustin, M. S.: Gaseous elemental mercury exchange with low mercury containing soils: Investigation of
530   controlling factors, Appl. Geochem., 22, 1451-1466, 10.1016/j.apgeochem.2007.02.006, 2007.

531 Yu, G., and Sun, X.: The principle and method of terrestrial ecosystems flux observations. Higher Education Press, Beijing,
532   2006. (In Chinese)

533 Zhang, H., Lindberg, S. E., Marsik, F. J., and Keeler, G. J.: Mercury air/surface exchange kinetics of background soils of the
534   Tahquamenon River watershed in the Michigan Upper Peninsula, Water Air Soil Pollut., 126, 151-169,
535   10.1023/a:1005227802306, 2001.

536 Zhang, H., Lindberg, S. E., and Kuiken, T.: Mysterious diel cycles of mercury emission from soils held in the dark at constant
537   temperature, Atmos. Environ., 42, 5424-5433, 10.1016/j.atmosenv.2008.02.037, 2008.

538 Zhang, L., Wang, S., Wang, L., Wu, Y., Duan, L., Wu, Q., Wang, F., Yang, M., Yang, H., Hao, J., and Liu, X.: Updated
539   emission inventories for speciated atmospheric mercury from anthropogenic sources in China, Environ. Sci. Technol., 49,
540   3185-3194, 10.1021/es504840m, 2015.

541 Zhang, Y., Jacob, D. J., Horowitz, H. M., Chen, L., Amos, H. M., Krabbenhoft, D. P., Slemr, F., St Louis, V. L., and Sunderland,
542   E. M.: Observed decrease in atmospheric mercury explained by global decline in anthropogenic emissions, Proceedings
543   of the National Academy of Sciences of the United States of America, 113, 526-531, 10.1073/pnas.1516312113, 2016.

544 Zhao, X., Guan, D., Wu, J., Jin, C., Han, S.: Distribution of footprint and flux source area of the mixed forest of broad-leaved
545   and Korean pine in Changbai Mountain, Journal of Beijing Forestry University, 27, 17-22, 2005.

546 Zhu, W., Sommar, J., Lin, C. J., and Feng, X.: Mercury vapor air-surface exchange measured by collocated
547   micrometeorological and enclosure methods - Part I: Data comparability and method characteristics, Atmos. Chem. Phys.,
548   15, 685-702, 10.5194/acp-15-685-2015, 2015.

549 Zhu, W., Lin, C.-J., Wang, X., Sommar, J., Fu, X., and Feng, X.: Global observations and modeling of atmosphere-surface
550   exchange of elemental mercury: a critical review, Atmos. Chem. Phys., 16, 4451-4480, 10.5194/acp-16-4451-2016, 2016.

551

Atmospheric
Chemistry
and Physics
Discussions

552   **Table1.** Description of QYZ and HT experimental station

Station sites	QYZ	HT
Location	115º04'E, 26º45'N	109º45'E, 26º50'N
Administrative region	Guanxi town, Jiangxi province	Guangping town, Hunan province
Altitude (m)	30~60	280~390
Climate type	Humid subtropical monsoon climate	
Mean annual temperature (°C)[a]	18.6	15.8
Mean annual precipitation (mm)[a]	1361	1200
Vegetation type	*Pinus massoniana*	*Cunninghamia lanceolata*
Forest age	31	27
Canopy height (m)	16	14
Dominant soil type (Chinese soil name)	Udic Ferrisols (Red Earth)	Haplic Acrisol (Yellow Earth)
Organic matter content in surface soil (g kg^{-1})[a]	10~15	28.3
Soil pH[a]	4.52	3.85
Annual average GEM concentration (ng m^{-3}) [b]	3.64 ± 1.82	5.93 ± 3.16
Hg content in soil organic layer (ng g^{-1})[c]	76.2 ± 6.0	153 ± 28
Hg content in surface (0~5 cm) soil (ng g^{-1})[c]	42.6 ± 2.3	167 ± 32

553   [a] Data of QYZ and HT stations according to Gao et al. (2014) and Wang et al. (2009), respectively;
554   [b] Mean value of the measurements at the height of 25 m and 35 m at QYZ site, 22.5 and 30.5 m at HT site;
555   [c] Analyzed based on 18 samples using a direct Hg analyzer (DMA80, Milestone Inc., Italy).
556

Atmospheric
Chemistry
and Physics
Discussions

557

558   **Table 2.** Pearson's correlation coefficient between GEM flux over forest canopy and atmospheric GEM concentration or each environmental

559   factor.

Factors	Sites	Winter	Spring	Summer	Fall
GEM concentration	QYZ	-0.142**	-0.155**	0.014	-0.141**
	HT	-0.232**	-0.226**	-0.197**	-0.183**
Air temperature	QYZ	0.272**	0.166**	0.31**	0.298**
	HT	0.143**	0.121**	0.188**	0.135**
Air humidity	QYZ	-0.314**	-0.003	-0.293**	-0.339**
	HT	-0.101*	-0.149**	-0.246**	-0.255**
Wind speed	QYZ	0.159**	0.176**	0.162**	0.166**
	HT	0.119**	0.180**	0.106**	0.162**
Soil temperature	QYZ	0.025	0.165**	0.288**	0.175**
	HT	0.015	0.174**	0.253**	0.201**
soil moisture	QYZ	0.102**	-0.198**	0.03	-0.106**
	HT	0.001	-0.032	-0.003	0.034
Radiation	QYZ	0.628**	0.403**	0.401**	0.209**
	HT	0.265**	0.212**	0.313**	0.201**

560   * Significant at $p < 0.01$ level;
561   ** Significant at $p < 0.001$ level.
562

Atmospheric
Chemistry
and Physics
Discussions

563 **Table 3.** Comparison of the GEM flux (ng·m^{-2}·h^{-1}) from different the observations.

Vegetation type	Location	winter	spring	summer	fall	GEM con	method	Data source
Subtropical coniferous forest	Jiangxi province, China	5.49	5.25	8.09	7.86	3.64	AGM	QYZ site
	Hunan province, China	-3.62	0.83	4.40	-0.40	5.93	AGM	HT site
Mature hardwood	Tennessee, USA	–	–	10-330	–	2.23	MBR	Lindberg et al. (1998)[a]
Yang pine plantation		–	–	–	17-86	1.45	MBR	
Boreal forest	Lake Gardsjon, Sweden	–	–	1-4	–	2.02	MBR	
Deciduous forest	Connecticut, USA	–	–	21.9	–	1.34	REA	Bash and Miller (2008)[b]
	Coventry Connecticut, England	–	–	-1.54	–	1.41	REA	Bash and Miller (2009)
Meadow	Fruebuel，central Switzerland	4.1	-4.8	2.5	0.3	1.29	AGM	Converse et al. (2010)
		-2.9	-1.5	3.2	-3.0	1.29	MBR	

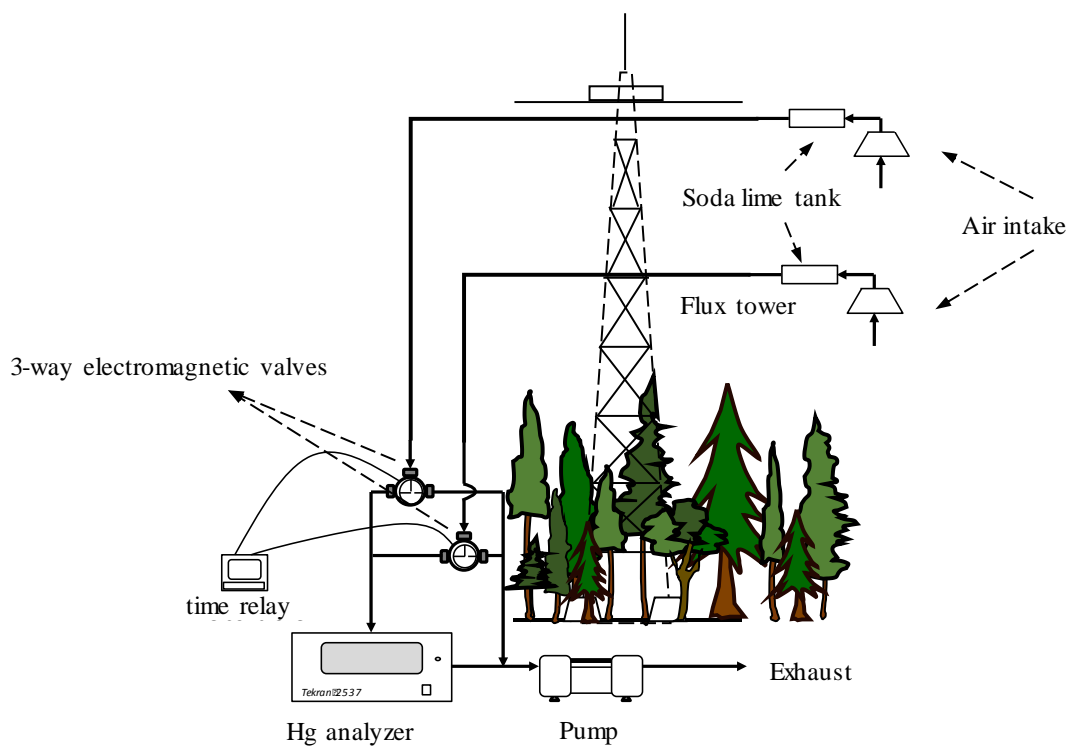564 [a] mean value (90% confidence interval), only measured during daytime;
565 [b] median value of TGM (total gaseous mercury) flux
566

567
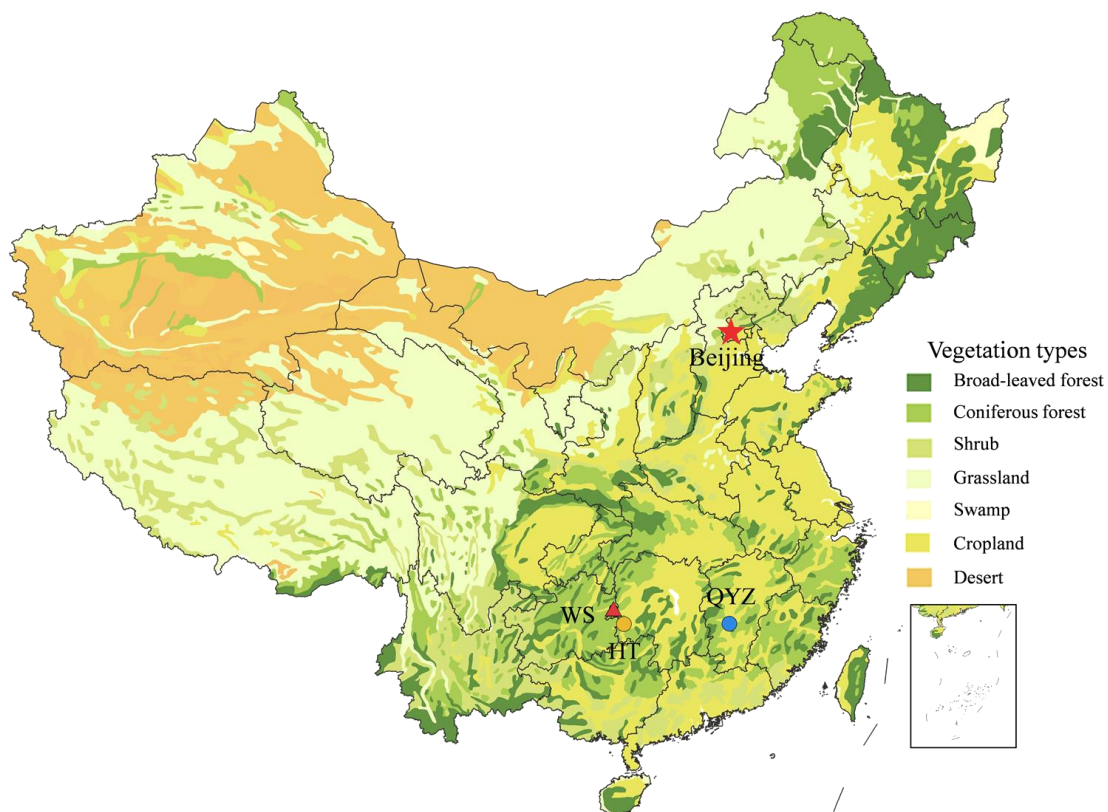
Figure 1: Locations of the QYZ station, HT station and WS Mercury Mine. Vegetation map of China (CAS., 2007) as background.
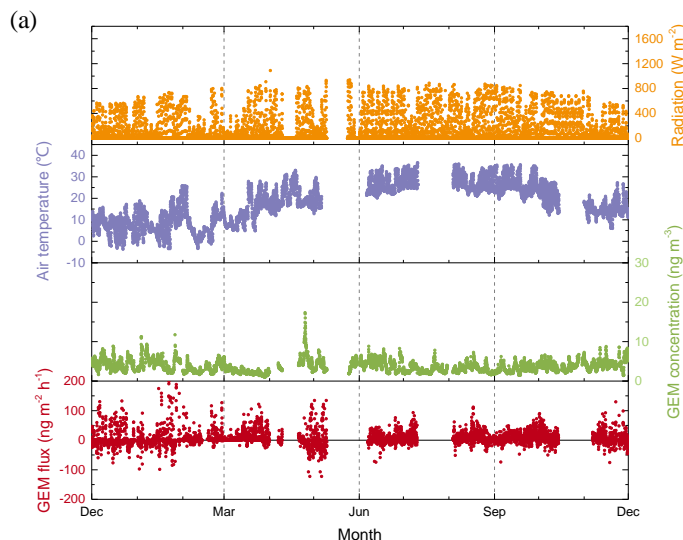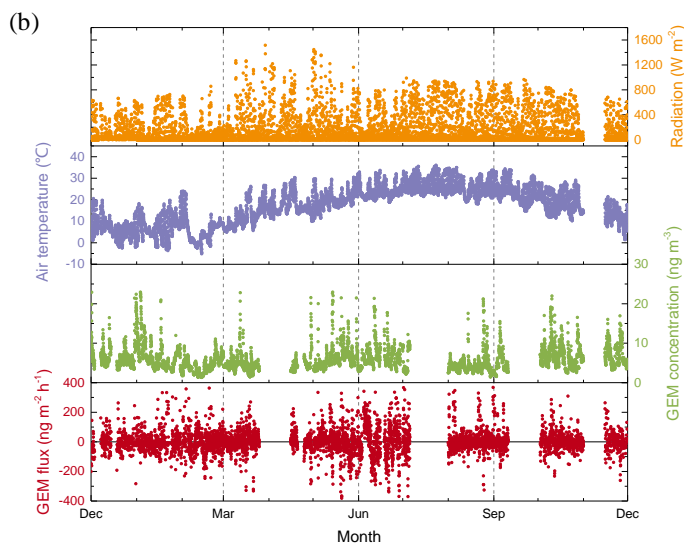
569

Atmospheric
Chemistry
and Physics
Discussions

570

Figure 2: Apparatus used to monitor vertical concentration gradient of GEM above forest canopy

572

(a)

573

(b)

574
575

576 **Figure 3: Hourly variations of solar radiation, air temperature, GEM concentration (the average value of the GEM concentration**
577 **at two heights), and GEM fluxes at QYZ (a) and HT (b) stations. The observations lasted for one year at both sites (January to**
578 **December in 2014). The data in April, May and December was supplemented with the data in 2013 due to the use of mercury analyzer**
579 **for measuring the soil and vegetation emission at HT site. Data loss were caused by elimination of the values outside the range of the**
580 **monthly mean ± 3 standard deviations, and the problematic data during the high atmospheric stability, instrument failure and**
581 **instability operation.**

582

Atmospheric
Chemistry
and Physics
Discussions

Open Access

EGU

583
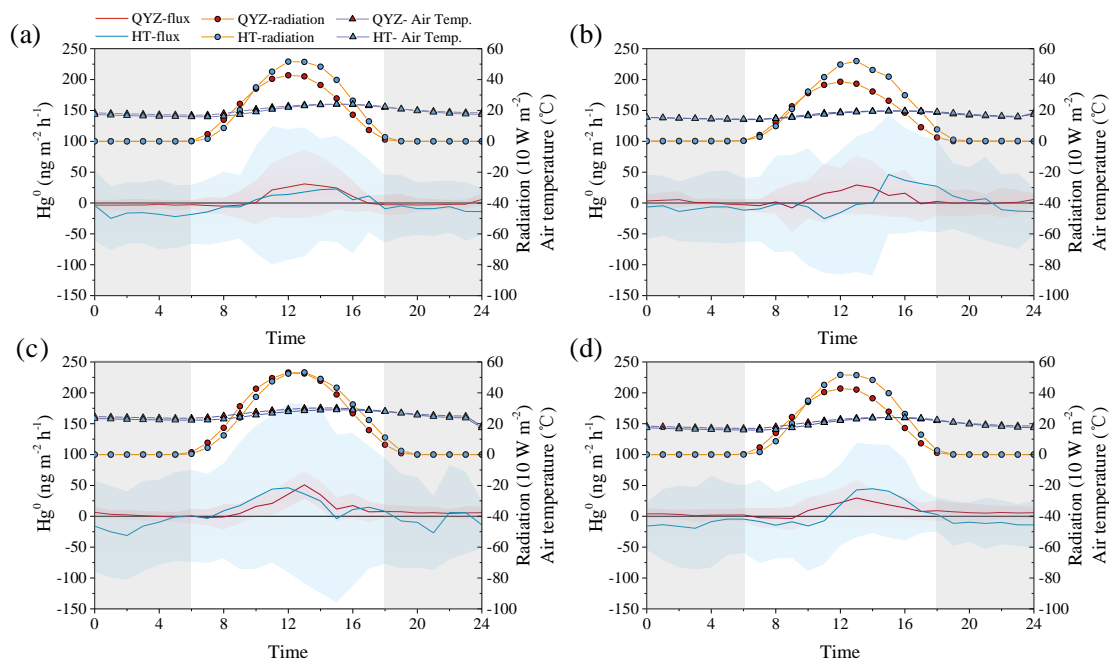
Figure 4: Diurnal variation in GEM fluxes, air temperature and solar radiation over forest canopy in each season. (a) Winter:

December to February; (b) Spring: March to May; (c) Summer: June to August; (d) Fall: September to October. Lines and

**envelopes depict mean values and standard variances.**

587

588
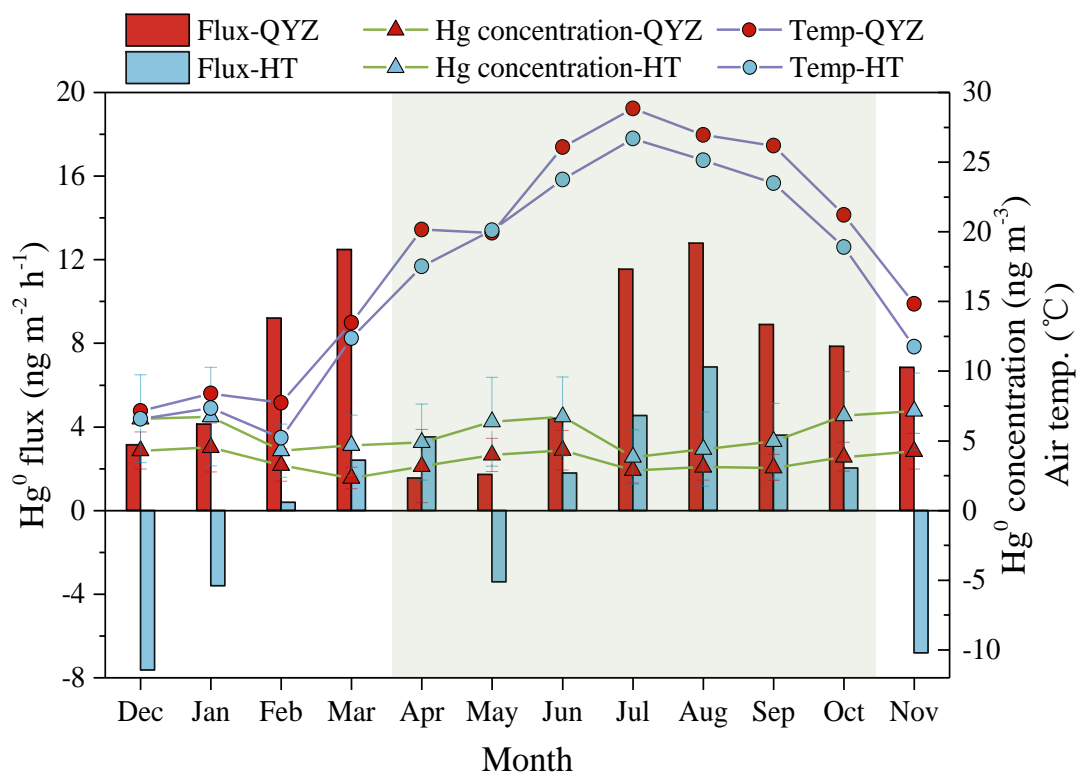
Figure 5: Monthly variations of GEM flux, GEM concentration and air temperature at QYZ and HT sites. Leaf-growing season

was marked as the shaded area.

591

Atmospheric
Chemistry
and Physics
Discussions

592
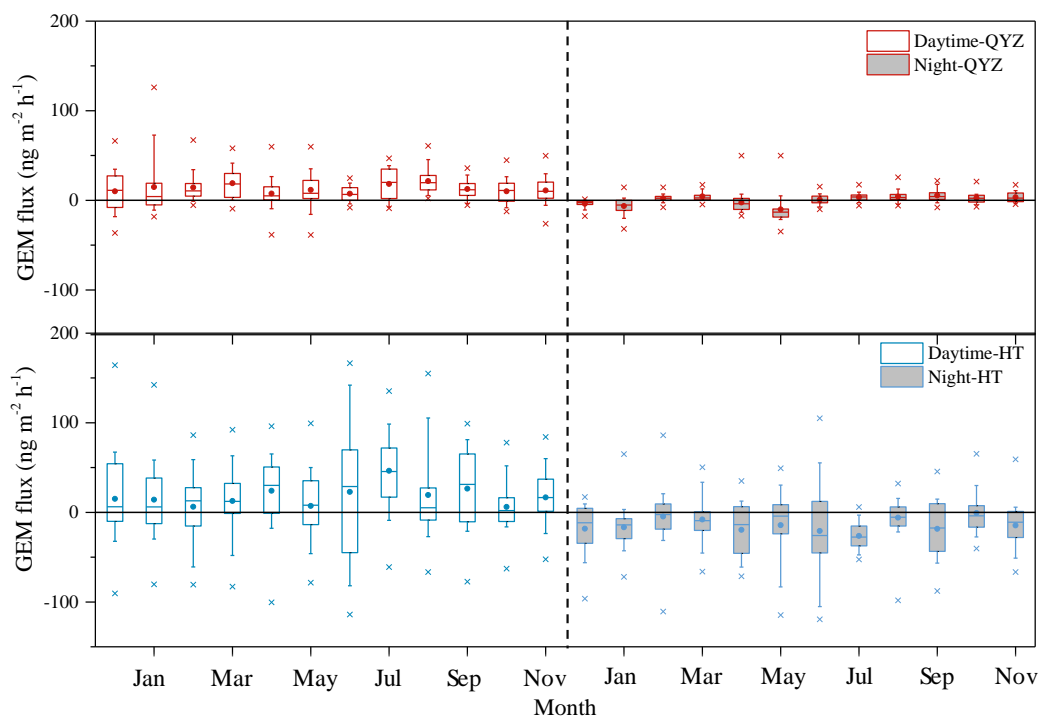
Figure 6: Monthly variation in daytime GEM flux (upper panels) and night GEM flux (under panels) during the measurement

periods at QYZ (a) and HT (b) sites. Box horizontal border lines represent the 25th, 50th and 75th percentiles from bottom to top,

the whiskers include the 10th and 90th percentiles, and the outliers (cross) encompass the minimum and maximum percentiles. The

solid circle in the box represents the mean value.

597

Atmospheric
Chemistry
and Physics
Discussions

598
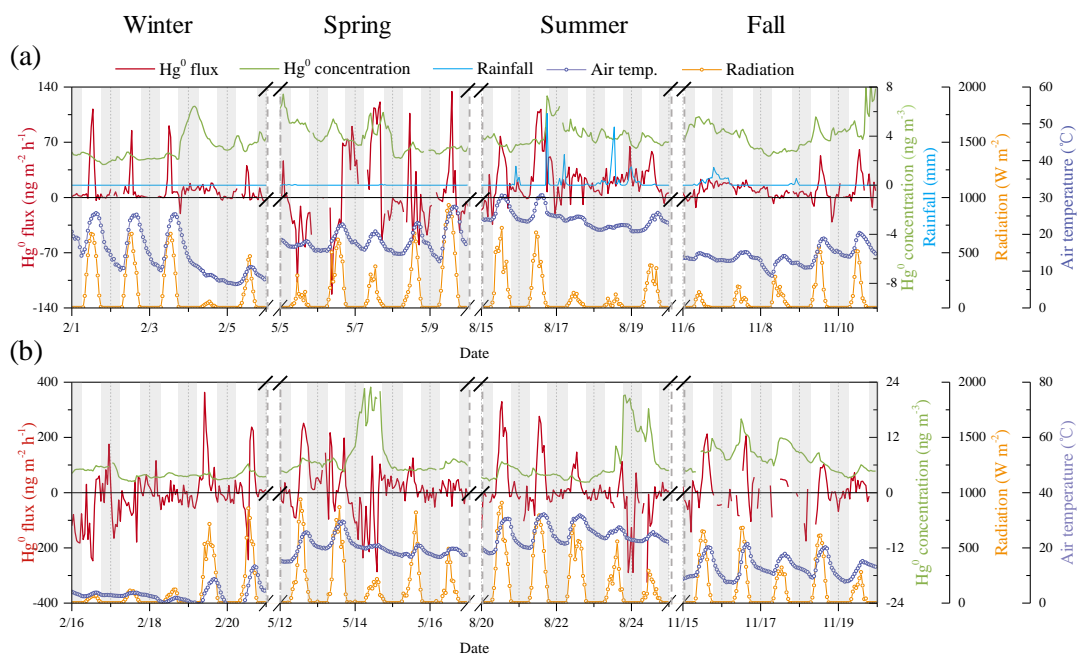
Figure 7: The GEM flux, concentration and environmental conditions in some typical days in each season at QYZ (a) and HT (b)

sites. Dates refer to China Standard Time (major ticks indicate midnight). All the data were indicated one-hour average.

601